1-1-1976

Growth of curved Al-CuAl2 ingots.

Verma Ravinder

GROWTH OF CURVED Al-$CuAl_2$ INGOTS

by

VERMA RAVINDER

A Thesis

Presented to the Graduate Committee

of Lehigh University

in Candidacy for the Degree of

Master of Science

in

The Department of Metallurgy and Material Science

Lehigh University

1976

CERTIFICATE OF APPROVAL

This thesis is accepted and approved in partial fulfillment of the requirements for the degree of Master of Science.

April 30, 1976
(Date)

Professor in charge

Chairman of Department

ACKNOWLEDGEMENTS

The author wishes to express his sincere appreciation to his advisor, Dr. R. W. Kraft for his guidance and patience throughout the course of this research and for his assistance in the preparation of this manuscript. Appreciation is also expressed to Dr. M. R. Notis.

The author wishes to thank the machine shop and the technicians in Whitaker Laboratories for their cooperation. Special thanks are given to fellow graduate students for their enlightening discussions and practical assistance.

Finally the author acknowledges the financial support from NASA Grant NCR 39-007-007.

TABLE OF CONTENTS

LIST OF FIGURES

ABSTRACT

The influence of ingot curvature on the morphology and crystallography of the Al-$CuAl_2$ eutectic alloy was invesitgated. Curved ingots of Al-$CuAl_2$ were grown by rotating a mold on a radius arm through a resistance furnace. After about 2 cms. of growth large single grains of the eutectic, with a lamellar structure, became stabilized and persisted for about 6 cms. of additional growth. The relative crystallographic orientation between the phases, as observed by transmission electron microscopy was determined as

$$\text{Zone } [0\ 1\ 1]_{Al} \ \| \ \text{Zone } [0\ \bar{1}\ \bar{1}]_{CuAl_2}$$

$$(1\ 1\ \bar{1})_{Al} \ \| \ (2\ 1\ \bar{1})_{CuAl_2}$$

This relationship remained unchanged at different positions in the curved ingots. The eutectic grains accommodated to curved growth and the lamellar structure and crystallographic relations were identical to those observed in linear ingots. The mechanisms of accommodation were related to lamellar faulting and the misorientations between the sub grains within the eutectic grain.

It was observed that the structure, i.e. both metallographic and crystallographic twisted about the ingot centerline along the length of the ingot. The habit plane did not coincide with any low index plane but was about 5° from $(1\ \bar{1}\ 1)_{Al}$ and $(2\ \bar{1}\ 1)_{CuAl_2}$.

INTRODUCTION

A. General Review

In recent years a significant amount of research work has been devoted to the structure and properties of directionally solidified eutectic alloys. It was in 1909 that Rosenhain and Tucker (1) observed the regular lamellar structure of Pb-Sn eutectic alloy and noted that "...one or both of the constituents are arranged in some definite crystalline manner throughout the grain." Today various theories, at different levels of sophistication, have been proposed regarding the structure, crystallography and classification of eutectic alloys. Several good review articles summarize these studies (2, 3, 4, 5).

At the same time several investigators began to examine some of the properties, both mechanical and physical, that could be obtained using directionally solidified eutectic alloys (6,7,8,9). Physical properties (viz, electrical, magnetic, optical and thermal) have been discussed in recent years in a number of review articles (10,11,12). Directionally solidified composites possess extremely attractive mechanical properties as compared to conventional materials. Probably the major potential use of such alloys is for high temperature applications, specifically for aircraft turbine blades. The high thermal stability, enhanced creep life, high fatigue and tensile

strength of certain classes of such composites have made them very promising new materials.

Most of the research on directionally solidified eutectics has been directed towards straight specimens formed by translating an alloy linearly through a temperature gradient. This was necessary to simplify not only the experimental set up but also to facilitate the understanding and interpretation of the factors governing the morphology and properties of these alloys. Very little work has been carried out on more complex shapes. However, even in the major projected use of structural eutectics--turbine blades--the shape is very complex and the growth process may be intentionally non-linear or non-intentionally non-linear near discontinuities. For example, in the attempt by L. D. Graham (13) to solidify turbine blades using investment casting molds, there were problems of misalignment of the phases with respect to the blade axis and structural irregularities were present at the root and shroud. This draws into prominence the need to study non-linear eutectic growth.

Before reviewing the work that has been done on non-linear eutectic growth it would be appropriate to discuss the factors influencing the structure of eutectic alloys.

B. Factors Influencing the Structure of Eutectic Alloys

Most of the eutectic alloys being used today freeze with either a lamellar or a rod type structure. The factors

influencing the morphology and the transition from lamellar to rod type structure are discussed briefly below.

1. Volume fraction of the two phases.

In steady state eutectic growth the interphase spacing, λ, is determined by the tendency to minimize λ, in order to reduce the diffusion distance at the solid liquid interface, and to increase λ so that the solid-solid interfacial area (and therefore the energy per unit volume) is reduced. The lamellar and fibrous morphologies are both favoured by the diffusion condition, and the preference for lamellae or rods depends on the solid-solid interfacial energy, which in turn is dependent on the relative volume of the two phases (14, 15, 16). This was expressed graphically by Cooksey (17), fig. 1, where volume fraction $V = \frac{V_\alpha}{V_\alpha + V_\beta}$, is plotted versus the interfacial area per unit volume (V_α and V_β are the volume fractions of the two phases α and β). The graph shows that if the α/β surface energies are equal, the fibrous morphology should be favoured for $V < 0.28$, and lamellar for $V > 0.28$. The figure 0.28 is not a precise one but serves to illustrate the role of volume fraction.

2. Growth rate (R) and temperature gradient (G).

It has been experimentally shown (18, 19, 20) that the lamellae to rod transition is encouraged in some eutectics by either a high growth rate or a low temperature

gradient. Cooksey (21) suggested that a low G/R ratio effectively increases the d/λ ratio. (d is the distance by which one phase leads the other at the solid-liquid interface.) The lamellar morphology becomes unstable when some critical lead distance is exceeded, but a stable isothermal interface can be retained by changing to the fibrous morphology. This tends to reduce the diffusion distance for the same interphase spacing.

3. Impurity concentration under cooling.

Experimental evidence has shown that the prevalence of the fibrous morphology tends to increase with an increase in the impurity content of the eutectic alloy (22, 23). Chadwick (22) suggested that if a given impurity has a different distribution coefficient, K, with respect to each solid phase, a constitutional undercooling effect will operate. This effect will induce the lamellae with the smaller K to break down into fibers. This theory was modified by Day and Hellawell (24), and Hunt (25) who suggested that the relative rates of rejection of the third component from each phase should be at least an order of magnitude lower than for the two components themselves.

4. Non-linear growth of eutectics.

Weart and Mack (c.r. 26,27) directionally solidified a number of eutectic alloys and demonstrated the existence of the colony structure. They showed that the bending of the lamellae close to the colony boundaries could cause the

breakdown of the lamellar structures.

Hunt and Clinton (15) studied the transition from lamellae to rods in various eutectic systems in the absence of impurities. They unidirectionally solidified high purity eutectic ingots in a graphite boat containing a graphite insert, as shown in Fig. 2. The ingots solidified with a plane interface until the tip of the insert was reached, then the solid liquid interface was forced to curve. In the five lamellar systems they studied, it was observed that some grains continued growing, but others broke down to a rod-like structure. In the grains that broke down, the lamellae lay parallel to the edge of the insert and would have had to bend sharply in order to remain normal to the interface. The grains in which the lamellae lay normal to the insert edge continued to grow with a lamellar structure. In the former grains the low energy interface is lost as a result of the lamellae bending sharply out of their own plane.

In general the transition from lamellar to rods is likely to occur whenever the solid-liquid interface becomes curved. Examples of this are observed when impurity cells are formed or the eutectic grain grows past an obstacle.

Jaffrey and Chadwick (29) in their attempt to study non-linear eutectic growth, solidified Al-Al_3Ni eutectic ingots. The general shape of these ingots was, as they described it, hook shaped (Fig. 3), with a stem 12 cms.

long and a cross section of 1 sq. cms. The curved region had a 9 cm. radius of curvature. They found that the minor Al_3Ni phase closely followed the local heat flow direction. The orientation of the Al_3Ni phase altered during the non-linear region in such a way that the growth direction was always [0 1 0]. During the growth of the hook-shaped crystals the two phases showed no tendency to develop a preferred orientation relationship. Garmong et al (30) and other investigators(28,31,32)in their studies on unidirectionally solidified straight Al-Al_3Ni linear eutectic ingots found a unique crystallographic relationship.

Growth direction $||$ $[0\ 1\ 0]_{Al_3Ni}$ $||$ $[0\ 1\ 1]_{Al}$

and $\{1\ 0\ 2\}_{Al_3Ni}$ $||$ $\{1\ 1\ 1\}_{Al}$

They attributed Chadwick's results (29) to the fact that the hook-shaped crystals had been grown horizontally whereas the linear crystals had been grown vertically. However, the very shape of the hook-shaped crystals resulting in non-linear growth could have been the cause of the difference in results.

Garmong (33) studied the structure and crystallography of Al-$CuAl_2$ and Al-Al_3Ni eutectic alloys by rotating a mold on a radius arm through an induction furnace. The solidified eutectic ingots were curved, comprising the

major part of a circle 25.4 cms. in diameter. The experimental set up was such that the solid-liquid interface was horizontal. For both systems, Garmong found that a preferred orientation between the phases develops early in the growth process and remains unchanged at different sections of the curved ingots. The relative orientation between the phases was the same as that found in linearly grown ingots. However, the lamellar habit plane was misoriented by about 6 to 8^{o} with respect to the usual crystallographic relation, viz

$$\text{interface} \;||\; (2\ 1\ \bar{1})_{CuAl_2} \;||\; (1\ \bar{1}\ 1)_{Al}$$

Garmong explained this observation in terms of regions of good fit separated by diffusion glide ledges (34).

C. Purpose of this research

Since, as pointed out, a majority of the eutectic studies have been concerned with straight specimens formed by translating an alloy linearly through a temperature gradient, this investigation was carried out to further our knowledge of eutectic growth in non-linear shapes. In this study, the Al-$CuAl_2$ system was selected because of its relatively low melting point and the copious literature available. The solidified eutectic ingots were curved in shape (Fig. 4) comprising the major portion of a circle 6.9 cms. in radius. This shape is similar to the curved ingots studied by Garmong (33), but the radius or curva-

ture in this investigation (6.9 cms.) is much sharper than the radius of curvature (12.7 cms.) of the ingots studied by Garmong. The purpose of choosing the smaller radius was to determine whether the radius of curvature of the ingot is critical to the structure and crystallography of the curved ingots. Standard microscopic procedures and transmission electron microscopy were used to study the changes in the structure and crystallography along the length of the directionally solidified curved eutectic ingots.

EXPERIMENTAL PROCEDURES

A. Master heat preparation

The starting materials were 99.99^{+}% Al and 99.999^{+}% Cu. In order to remove surface impurities the aluminum was cleaned with acetone and the copper with acid. Following the cleaning the metals were accurately weighed on a Mettler Balance to obtain the desired composition. An average master heat weighed about 800 grams.

The charge was placed in an alumina crucible and melting was carried out in a vacuum induction furnace under a positive pressure of argon. The melt was superheated to about 950°C, to assure good mixing, cooled to 800°C and cast into a split metal mold which yielded 8 cylindrical blanks about 30 cms. long and 1.27 cm. in diameter.

B. Preparation of curved eutectic ingots

The cylindrical blanks were remelted in a small alumina crucible and poured into toroidally shaped split graphite molds. Fig. 4 shows the mold and a cast curved eutectic ingot. The radius of curvature of the ingot centerline was 6.9 cms. with a circular cross section of 1.25 cms. Ultra high purity graphite obtained from Ultra Carbon Corporation was used in the preparation of the molds.

C. Directional Solidification

The cast eutectic ingots were placed in a split graphite mold. The two halves of the mold were wired together. The mold assembly was passed through a specially constructed resistance furnace. The furnace and the crucible assembly were housed in a box (Fig. 5) with provisions made to pass argon through the box to minimize oxidation of the crucible. A water quenching device (not shown in Fig. 5) cooled the crucible as it left the furnace in order to increase the temperature gradient at the solidifying interface.

As the system was designed to operate in an inert atmosphere the drive mechanism was placed outside the assembly. The crucible assembly was moved through the furnace by means of a drive drum powered by a conventional zone melting apparatus via a flexible cable wound around the drum. The crucible assembly could be rotated through the furnace at linear speeds ranging from 1.25 to 50 cms. per hour.

The apparatus was constructed so that solidification proceeded vertically downwards. The solid liquid interface was in the horizontal plane, the liquid phase being on top of the solid as solidification progressed.

D. Metallography

In order to fully understand eutectic growth in curved shapes, it was necessary to determine the orienta-

tion of the lamellae and the crystallographic relations between the phases at different positions in the ingot.

Locations in the ingot are specified in degrees from the head end of the ingot. A sample for microstructural and/or crystallographic examination may be described as prepared from a transverse section at $\theta = 15°$, or a grain might extend from $\theta = 15°$ to $\theta = 65°$.

In order to correlate the metallographic and the crystallographic data with position in the ingot it was necessary to set up a master coordinate system, shown in Fig. 6. The X axis corresponds to the radius vector, the Y axis to the axis of the curved ingot, and the Z axis is perpendicular to the above two. From Fig. 6 it is clear that X and Y axis change for successive sections but the Z axis remains the same.

Longitudinal and transverse sections were prepared as needed. At least four sections, at different θ values were examined in each ingot. Sections were cut from the solidified ingots using an Electron Discharge Machine. Table I lists the positions of the sections, in terms of angle θ and distance from the head end, for the two ingots that were examined in detail.

Specimens were prepared for microscopic examination by grinding through 600 grit paper, polishing with Linde A and etching with Keller's Reagent (95 ml. H_2O, 1 ml. HF, 1.5 ml. HCl, and 2.5 ml. HNO_3) for 25 to 30 seconds.

In order to determine the orientation of the lamellae, a two surface analysis was carried out on the transverse sections and the longitudinal sections (35). As shown in Fig. 7 a flat was ground on the ingot and the angle made by the lamellae trace with the Z axis, $\emptyset$, and the X axis, ψ, was measured. These angles are listed in Table I. The measurements were made using a light microscope with a rotating stage. At least five readings were taken on each section.

E. Transmission Electron Microscopy

Using the Electron Discharge Machine, circular blanks, 2 mm. in diameter, were cut from the transverse sections, for examination in the Transmission Electron Microscope. To aid in determining the orientation of the specimen relative to the ingot, the side of transverse section facing the head end of the ingot was marked with a small quantity of a lacquer, Microstop.

The circular discs were jet polished with an electrolyte that was a mixture of water, acetic acid, phosphoric acid and nitric acid (4:3:2:1). The voltage used was 60 V and the discs were jet polished for 40 seconds at room temperature.

The discs were then electropolished using an electrolyte consisting of 70% methanol and 30% nitric acid at 40 V and -80°C. The temperature was attained using a liquid nitrogen bath surrounding the electrolyte. The polish-

ing was carried out until a small hole appeared in the discs. The samples were stored in methanol under vacuum. A Philips EM300, 100KV transmission electron microscope was used.

RESULTS AND DISCUSSION

A. Solidification and Metallography

During the course of this investigation considerable time was devoted to controlling the growth rate and the temperature gradient in order to obtain a lamellar structure consistently. Based on this work a growth rate of 2.5 cms. per hour and a temperature gradient between 45 and 50°C per cm. were selected.

Macroscopically, the structures obtained in the curved eutectic ingots were similar to those found in linear ingots. At the head end of the ingot where solidification initiated, a zone about 2 cms. long containing a large number of fine grains was present. By about $\theta = 10°$, most of these grains had disappeared and a long single grain region was observed. In one ingot grown at 2.5 cms. per hour a single grain was present from $\theta = 15°$ to $\theta = 65°$, in another from $\theta = 24°$ to $\theta = 78°$. In these regions there was no evidence of any high angle boundaries.

In the two ingots selected for detailed examination, transverse sections in the single grain region revealed a typical lamellar structure under a light microscope. There was no marked difference between this structure and the lamellar structure obtained in linear ingots. Fault boundaries are present here as in linear ingots. The mismatch surfaces present formed a sub structure within the

eutectic grain. It was observed that most faulted regions persisted for some distance and that some new ones were continually being formed. Within the last few centimeters of growth a distinct colony structure was seen in both the ingots studied.

B. Rotation of the structure

The transverse sections of the two curved ingots selected for detailed study lay in the region where a large single grain predominated. Two surface analysis was carried out on at least four different sections for both the ingots. (Table I)

In Fig. 7, the angle $\emptyset$ is plotted against distance in the growth direction for the two ingots. From Fig. 7 it can be inferred that the lamellar planes twisted around the Y axis during growth in a helical manner. The lamellar rotation rate was computed and was nearly constant for the two ingots--6 to 8°/ cm.

The angles $\emptyset$ and ψ measured in the two surface analysis were used to plot the positions of the lamellar traces and lamellar poles, at the different angular positions, onto a stereographic projection. Fig. 8 is such a projection for Ingot I. In this projection the center of projection was the axis of the curved ingot, i.e. Y axis, the top represents the Z axis which is fixed.

This projection showed that the lamellar traces on the transverse planes rotated around the axis of the curved

ingot along its length. Furthermore it can be seen that the sense of rotation is constant, i.e. a given grain does not rotate first clockwise, then counterclockwise. In this investigation, the sense of rotation was anticlockwise for both the ingots examined.

In order to understand this twisting phenomena it is useful to understand first the concept of a eutectic grain. A eutectic grain has been defined as that portion of a eutectic specimen in which the crystallographic orientation of each phase and the microstructure and metallographic orientation have fixed angular relations (36). From Fig. 8, it is clear that for a curved ingot, a fixed angular relation between the lamellar orientation and the growth direction is not maintained. In fact recent studies (34, 37, 38) on linear eutectic ingots have shown that during the growth of a eutectic grain, both crystallographic and metallographic relations may change progressively so that large changes in angle occur within a region in which continuous growth has occurred from a single nucleation site.

The rotation of the lamellae poles around the growth axis has been observed in certain systems (39, 40, 41). In fact the rate of rotation, 6 to 8°/cm. observed in the curved ingots, is in good agreement with the rate of rotation found by Double et al (39) in their study on linear ingots of Al-$CuAl_2$.

The reasons for this rotation phenomenon are not fully

understood but certain observations are pertinent. The rate of rotation is directly related to the perfection of the lamellar arrangement, i.e. to the subgrain density and the range of misorientations. In fact it has been observed (39, 40, 41) that the rate of rotation in a given system bears an inverse relationship to the ambient temperature gradient during growth, and that the temperature gradient is related to the degree of perfection of the lamellar arrangement. In this investigation the temperature gradient was the same for both ingots and consequently the same rotation rate was observed.

In the systems in which this rotation phenomena has been observed, it was seen that there were elements of asymmetry in the phase orientations and of the interface between the phases. This is discussed further in the next section on crystallographic relations.

C. Crystallographic relations

As stated earlier, transmission electron microscopic examination was used to determine the crystallographic relation between the two phases. The thin foils for the TEM were prepared adjacent to each metallographic section used in the two surface analysis.

Fig. 9 a,b,c, show the selected area diffraction patterns from the Al phase, the $CuAl_2$ phase, and the associated image respectively from the section of $\theta = 40°$ in ingot I. The selected area diffraction patterns were

rotated to correspond to the image. This was done by using the predetermined image diffraction rotation calibration for the electron microscope.

Within 2° the relative orientation relation between the two phases was determined as

$$\text{Zone } [0\ 1\ 1]_{Al} \ \| \ \text{Zone } [0\ \bar{1}\ \bar{1}]_{CuAl_2}$$

$$(1\ 1\ \bar{1})_{Al} \ \| \ (2\ 1\ \bar{1})_{CuAl_2}$$

This relation was found in all the samples that were examined from both ingots. The preferred orientation developed at the onset of the second zone and remained unchanged at the various angular positions for both ingots, i.e.the crystallographic directions followed the curvature. Fig. 10 illustrates the meaning of this statement. In Fig. 10 in the right section the crystallographic axis remains fixed in space, whereas for the left section the axis changes with specimen curvature. For the two ingots examined the crystallographic axes follow the curvature as in the left section in Fig. 10. These ingots can therefore be regarded as "single crystals."

The relative orientation between the two phases in the curved ingots, viz,

$$\text{Zone } [0\ 1\ 1]_{Al} \ \| \ \text{Zone } [0\ \bar{1}\ \bar{1}]_{CuAl_2}$$

$$(1\ 1\ \bar{1})_{Al} \ \| \ (2\ 1\ \bar{1})_{CuAl_2}$$

is the same as that observed in linear ingots (37, 39).

In order to understand the effect of curvature on the crystallography and metallographic structure, the data from the two surface analysis and the transmission electron microscope examination were combined onto a common sterographic projection. Fig. 11 shows such a projection for Ingot I. This projection was obtained in the following manner:

1. The diffraction patterns obtained at the different angular positions in the two ingots were rotated to correspond to their respective images. This was done by using the predetermined image diffraction rotation calibration for the instrument.
2. The average angle made by the lamellae trace on the transverse plane with the Z axis was known from the results of the two surface analysis. From the image of the lamellae in the TEM photographs and the above angle it was possible to fix the location of the Z axis on the photographs and consequently onto the diffraction directions.
3. The angles made by the diffraction directions $(2\ 1\ \bar{1})_{CuAl_2}$ and $(1\ 1\ \bar{1})_{Al}$ with the Z axis were measured. These angles were used to mark the positions of the $(2\ 1\ \bar{1})_{CuAl_2}$ and $(1\ 1\ \bar{1})_{Al}$ directions onto the sterographic projection. Fig. 11 shows the position of these diffraction directions

1, 2, 3, 4) and the lamellar poles (P_1, P_2, P_3, P_4) for Ingot I. Similar results were obtained for Ingot II.

The concept of a "single eutectic crystal" having a crystallographic orientation that varies with the specimen curvature seems to be paradoxical. To accomplish the change in the position of the crystallographic directions there has to be some degree of freedom from the rigid definition of the eutectic grain. In fact for many systems (37) it has been observed that although specific orientation relationships do exist between the phases it is only loosely preferred and small deviations do occur between adjacent lamellae. The diffraction patterns obtained in this investigation confirm this fact. Davies and Hellawell (37) studied the variation between the lamellae by tracing the movement of Kikuchi lines over a series of lamellae. They examined foils cut at right angles to and parallel to the growth axis. They found that rotations were larger on the longitudinal planes than on the transverse planes, i.e. rotational freedom is greater about axes closer to the growth axis rather than at right angles to it. Since there is some freedom from perfectly preferred configurations, different portions of the solid-liquid interface could be slightly out of phase in the sense of small divergences from the apparently ideal orientations. These phenomena can help in understanding how the crystallographic

directions vary with specimen curvature. The small variations in orientation lead to the formation of subboundaries and these variations can add up to accommodate the crystallographic variation. In the curved ingots it was seen that even though no high angle boundaries were present, there were a number of subgrains. Some of these subgrains persisted for some distance and new ones were continually being nucleated. It is proposed that the subgrains persist as long as they deviate slightly from the low energy configurations. As they become unfavorably oriented they are replaced by new subgrains which are of slightly different orientation and are more favorably oriented.

D. Lamellar Interface

In order to determine the nature of the lamellar interface the data from the projection shown in Fig. 11 were plotted differently in the projection shown in Fig. 12. The points representing the crystallographic relation $(2\ 1\ \bar{1})_{CuAl_2} \parallel (1\ 1\ \bar{1})_{Al}$ at the different Θ values in Ingot I were plotted as a single point, T, in the projection in Fig. 12. The lamellar poles P_1, P_2, P_3, P_4 were correspondingly rotated about the center of the projection Y. In addition to this the principal poles for the $CuAl_2$ and Al phases, all the $\{1\ 1\ 1\}_{Al}$ phases and the $\{2\ 1\ 1\}_{CuAl_2}$ phases were plotted.

As seen from Fig. 12, the lamellar poles lie about 70 - 75° from the plane described by the relation $(2\ 1\ \bar{1})_{CuAl_2} \parallel (1\ 1\ \bar{1})_{Al}$ but they lie close to the $(\bar{1}\ \bar{1}\ \bar{1})_{Al}$ and $(2\ \bar{1}\ 1)_{CuAl_2}$. The $(\bar{1}\ 1\ \bar{1})_{Al}$ plane is about 5° from $(2\ \bar{1}\ 1)_{CuAl_2}$. Similar results were obtained for Ingot II.

In the curved ingots, distinct crystallographic coincidence between the phases is present but the habit plane does not coincide with any low index plane. Yet, the lamellar habit plane is approximately preferred and lies close to $(1\ \bar{1}\ 1)_{Al}$ and $(2\ \bar{1}\ 1)_{CuAl_2}$.

The selection of the preferred interface plane is some complex function of the five degrees of crystallographic freedom of the interface. Studies have shown that the interface is generally a low energy interface and is parallel to crystallographic planes of wide spacing and nearly equal atomic densities (42, 43). This phenomenon conforms with the analysis by Fletcher and Adamson (44) which involves summing the interaction energies between adjacent atoms across the interface, taking account of their relative displacements (chemical energy) and summing the strain energies due to displacements of the atoms from equilibrium positions in their lattices. This analysis predicts that the surface energy between the two solid phases will vary when the relationship between the interfacial and crystal orientations is varied. The surface

energy can be plotted as contours in terms of the five configurational parameters. During the growth process the flexibility of the system allows it to seek out the valleys and the minima of the energy surface. The driving force for this is provided by the slope of the surface. There are bound to be several minima in such a complex problem, some of greater depth and sharpness than others. A sharp cusp would represent a rigidly preferred configuration and a shallow cusp a more loosely preferred configuration. The portions of the contour surface, close to the deep cusps, would confer relative stability to the group of lamellae with orientation slightly different from the preferred orientations. However, this growing crystal will experience a driving force encouraging a change of orientation characteristic of the bottom of the cusp. The mechanisms by which these changes would occur are related to the presence of faults and subboundaries in the lamellar structure. The extent to which these changes do take place depends on the crystallographic features of the alloy system and other constraints during growth. For the Al-$CuAl_2$ system it would seem that a shallow cusp exists as loosely preferred configurations are found.

For the curved ingots it was seen that the lamellar interface lies close to the $(\bar{1}\ 1\ \bar{1})_{Al}$ and $(2\ \bar{1}\ 1)_{CuAl_2}$. In order to understand how deviations from the loosely preferred low energy interface do not lead to a breakdown

of the structure it is necessary to consider a model of the lamellar interface. Using grain boundary models as a starting point Garmong (34) has proposed a boundary coincidence model. This model emphasizes the importance of atomic density matching and interfacial ledges. Arrays of diffusion glide ledges allow boundary misorientation with only slight modification of the preferred crystallographic relations. The broad faces between the ledges retain their low energy configurations. This model thus accounts for small deviations of the observed interfacial planes from the expected low energy orientation if the boundary can be assumed to contain the proper array of ledges. In fact Garmong (34) in his study on Al-$CuAl_2$ interface structure did find evidence of such ledges.

CONCLUSIONS

Eutectic alloys having a stable structure can be directionally solidified in curved shapes 6.9 cms. in radius where strictly linear heat flow conditions are not maintained. The radius of curvature of the ingot is undoubtedly critical to the microstructural and crystallographic relations.

In Al-$CuAl_2$ curved ingots, a lamellar structure is observed. The preferred crystallographic relations between the phases are

$$\text{Zone } [0\ 1\ 1]_{Al} \ || \ \text{Zone } [0\ 1\ 1]_{CuAl_2}$$

$$(1\ 1\ \bar{1})_{Al} \ || \ (2\ 1\ \bar{1})_{CuAl_2}$$

These relations are loosely preferred and remain unchanged at different positions in the curved ingots. The small variations in orientation lead to the formation of subboundaries which are slightly misoriented with respect to each other. These small variations can add up and permit the crystallographic relations to remain unchanged along the length of the curved ingots.

The structure, both metallographic and crystallographic, twists about the ingot centerline, along the length of the ingot. The rate of rotation of the lamellae is constant, 6 to 8°/cm., and is related to the perfection of the lamellar arrangement.

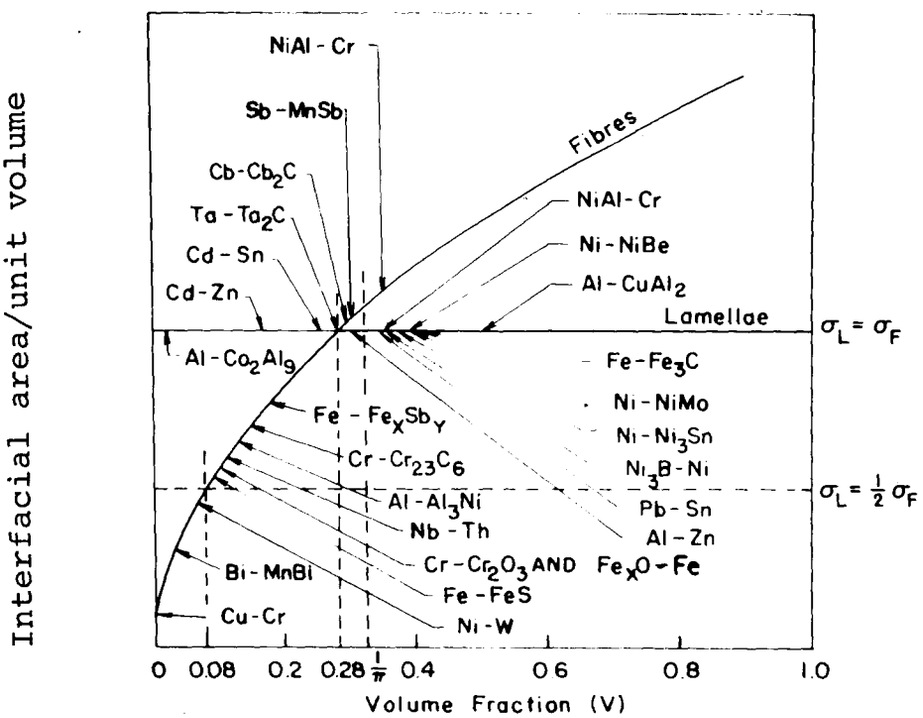

Fig. 1 Correlation between observed microstructures and volume fraction criterion. Cooksey (17).

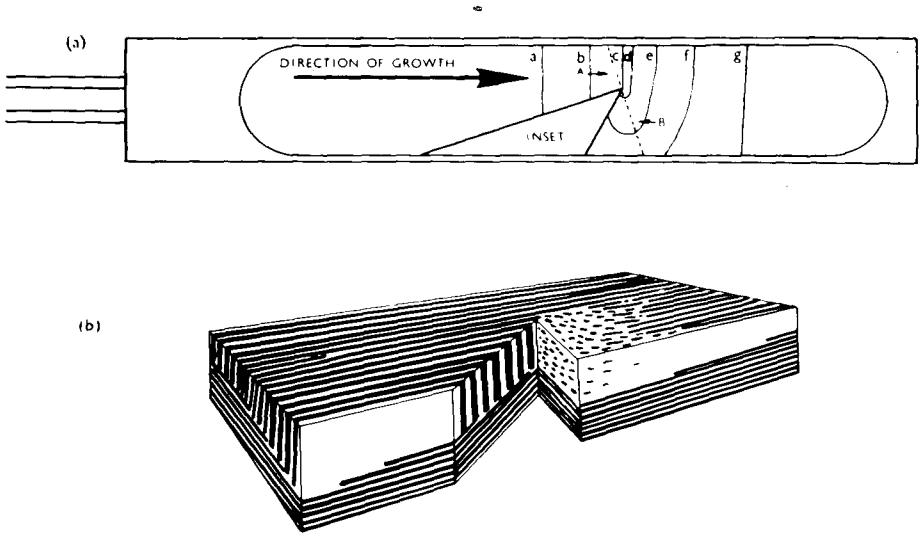

Fig. 2 (a) Plan of the boat, used by Hunt et al (15) in studying the bending of lamellae, showing the shape and position of the solid liquid interface at successive time intervals, a to g.

(b) A schematic illustration of two grains of a lamellar eutectic, one of which breaks down into a rod-like structure as the grain grows around the insert.

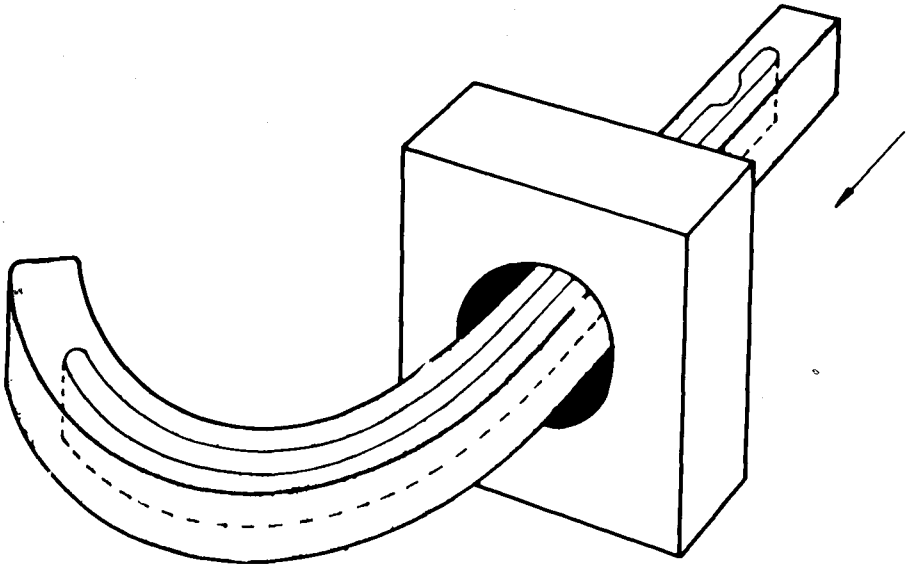

Fig. 3 Schematic representation of the arrangement used for the growth of hook-shaped Al-Al_3Ni ingots. Jaffrey and Chadwick (29).

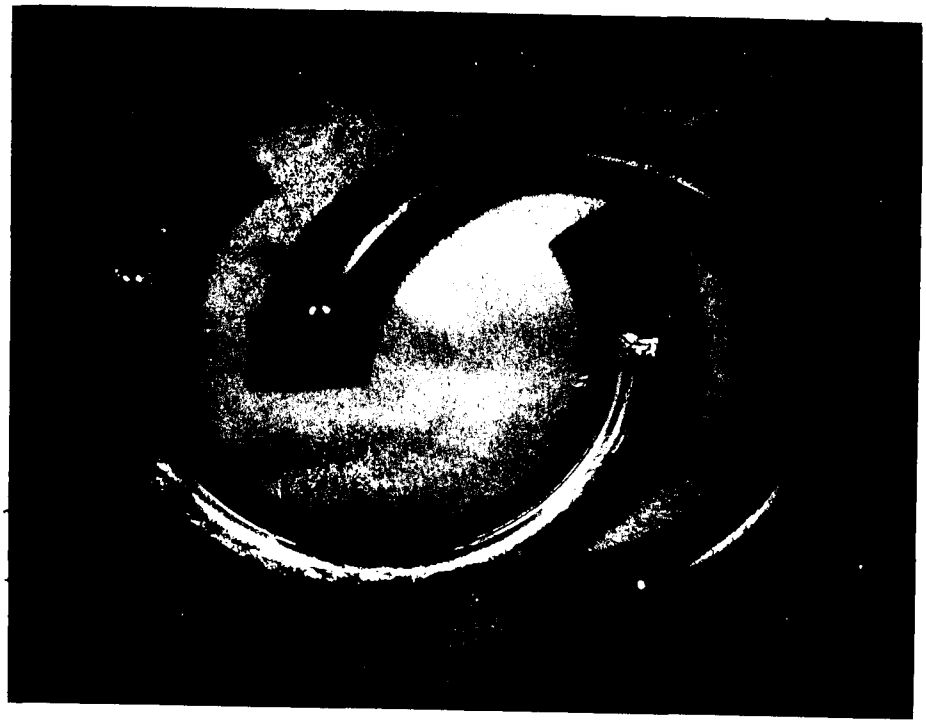

Fig. 4 Split graphite mold and specimen used in the growth of the curved Al-$CuAl_2$ ingots.

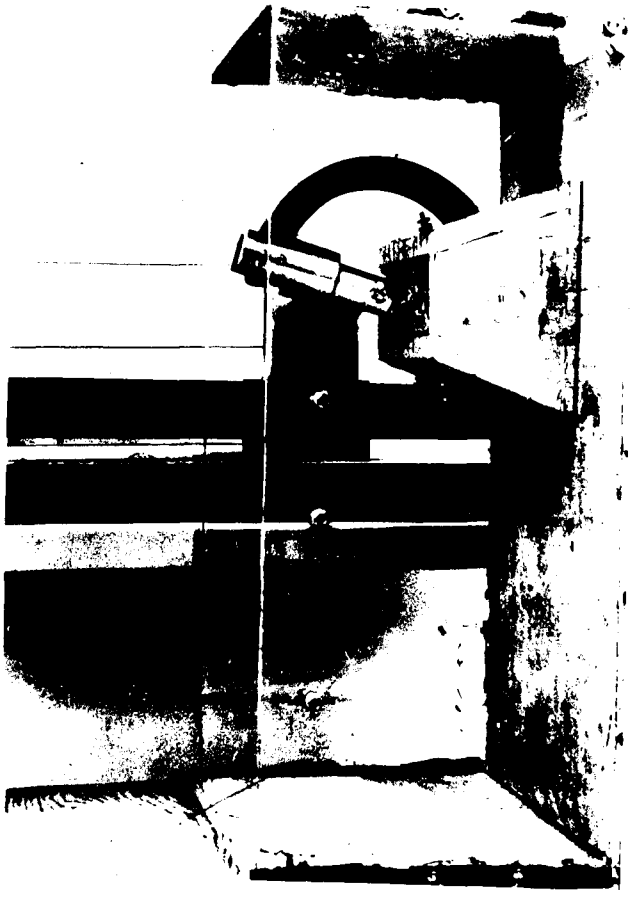

Fig. 5 Apparatus used in the directional solidification of curved eutectic ingots.

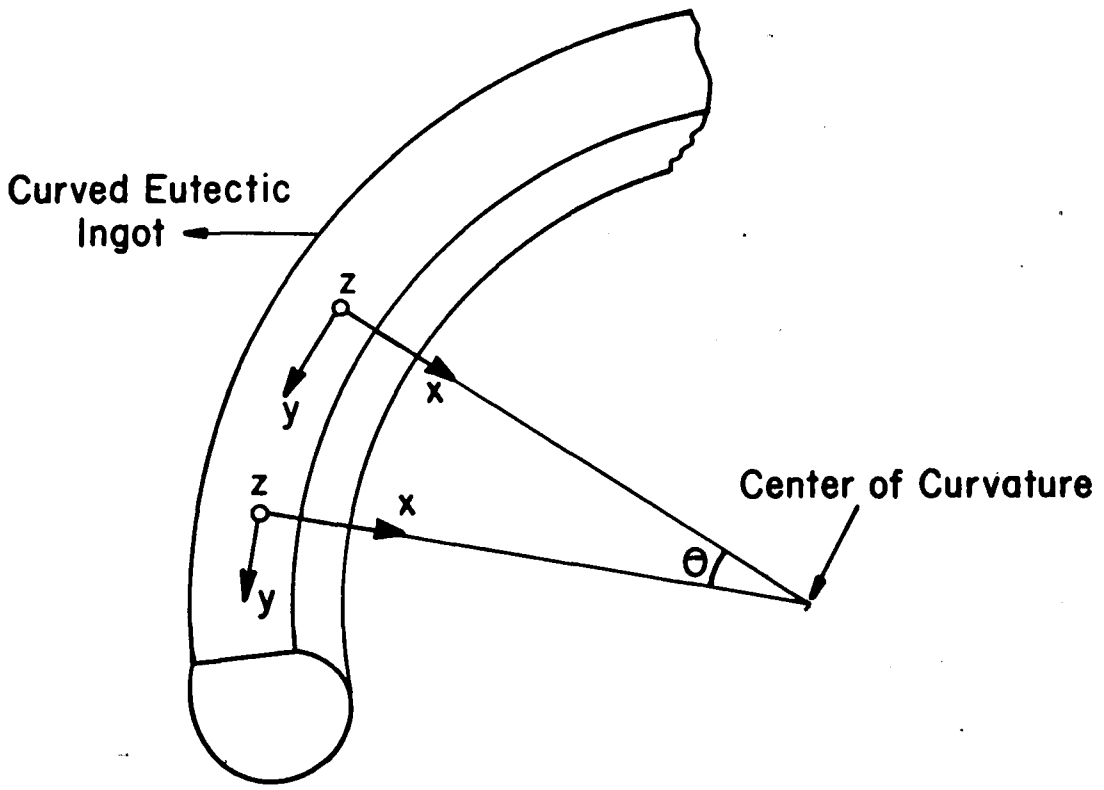

Fig. 6 Ingot sketch and coordinate system for the curved ingots.

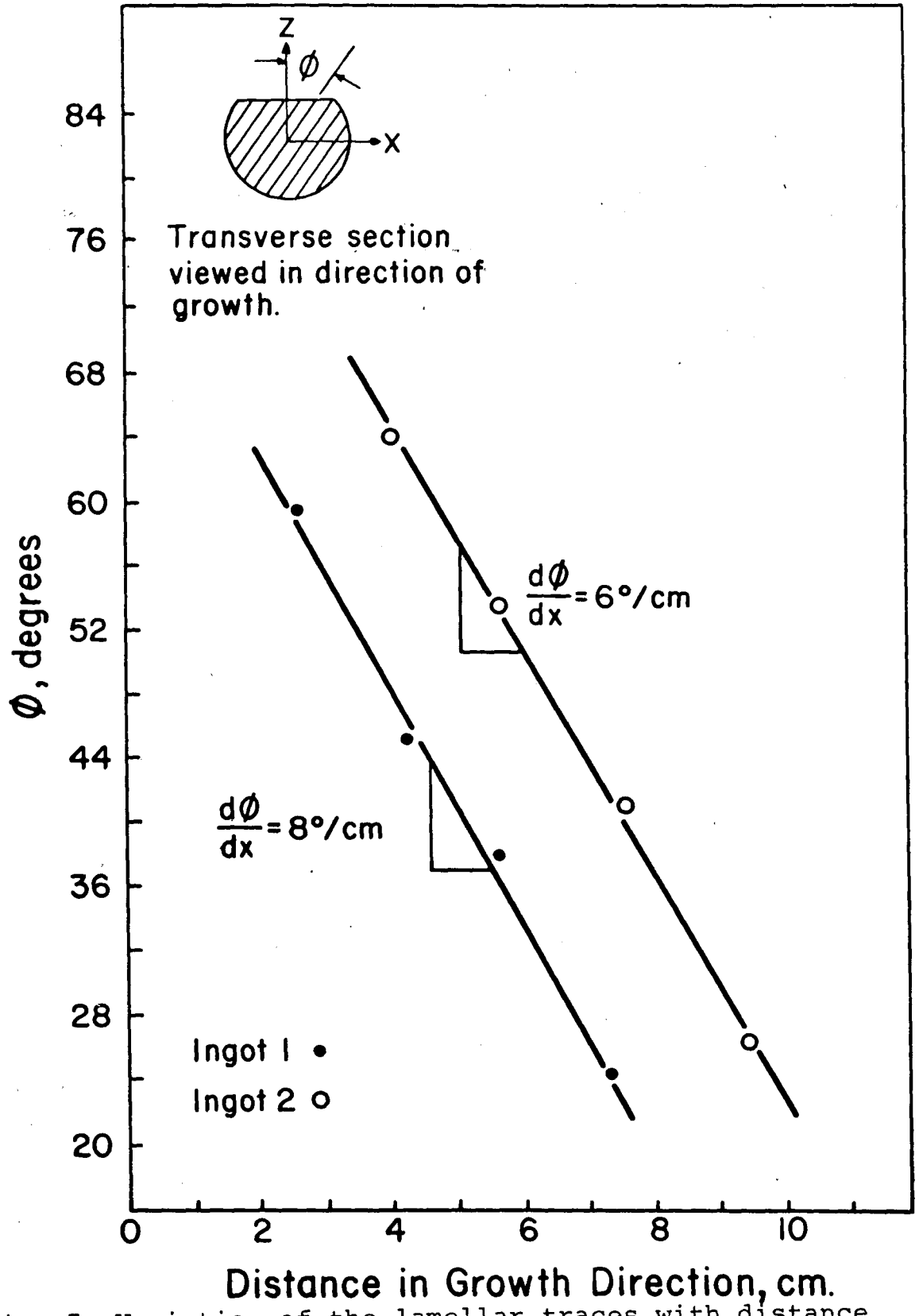

Fig. 7 Variation of the lamellar traces with distance along the length of the curved ingots.

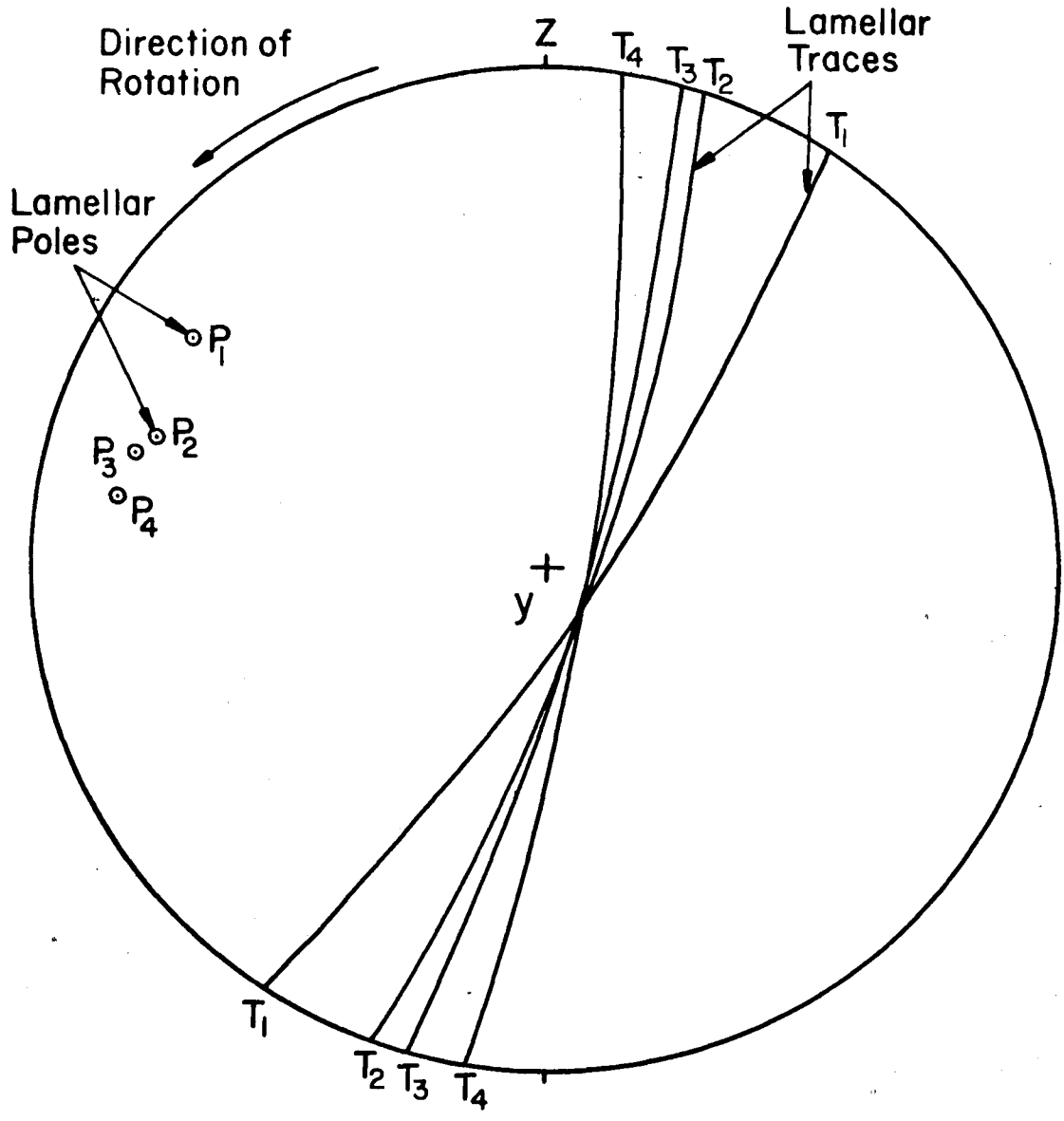

Fig. 8 Stereogram showing the lamellar traces and lamellar interface normals in Ingot I. The interface normals twist around the ingot axis Y.

Fig. 9 (a) Transmission electron micrograph of the transverse section of Ingot I at $\theta = 40°$, from which SAD patterns 9(b) and 9(c) [page 37] were obtained. Mag. 35000. Al is the light phase.

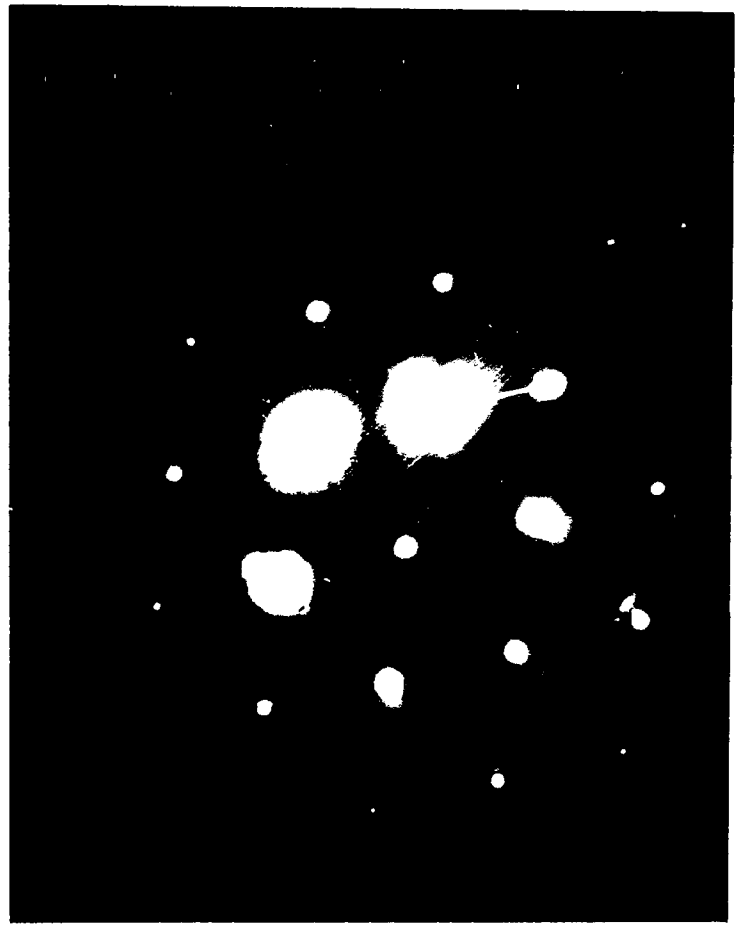

Fig. 9(b) Selected area diffraction pattern from Al phase.

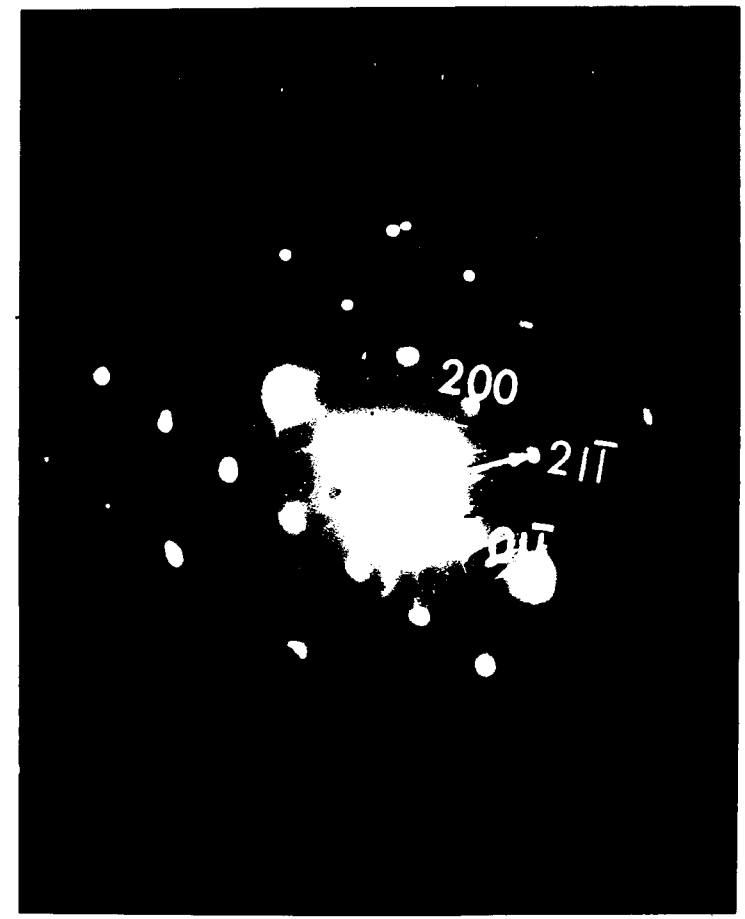

Fig. 9(c) Selected area diffraction pattern from $CuAl_2$ phase.

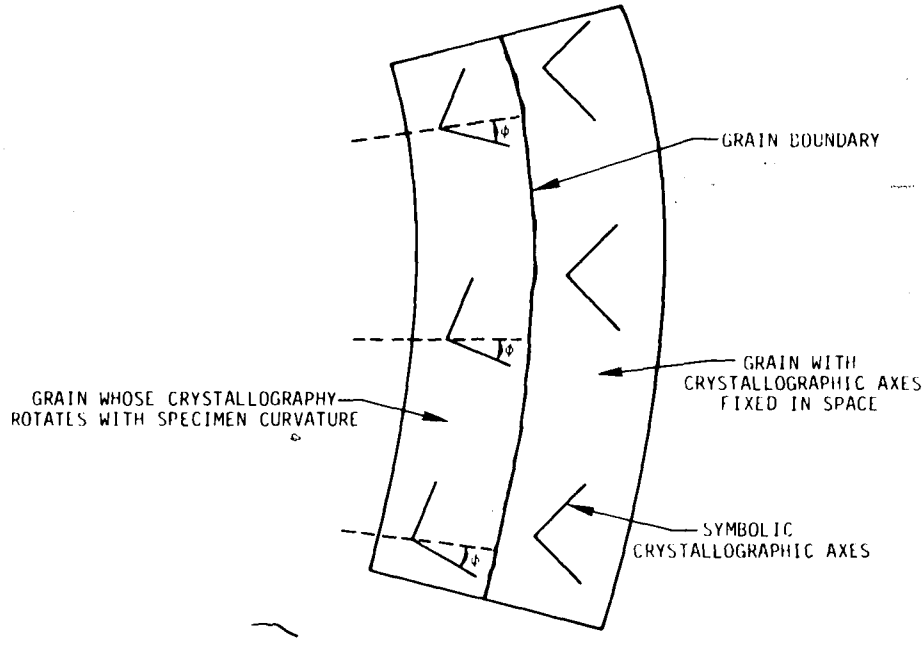

Fig. 10 Schematic representation indicating possible response of crystallographic axis to curved growth (33).

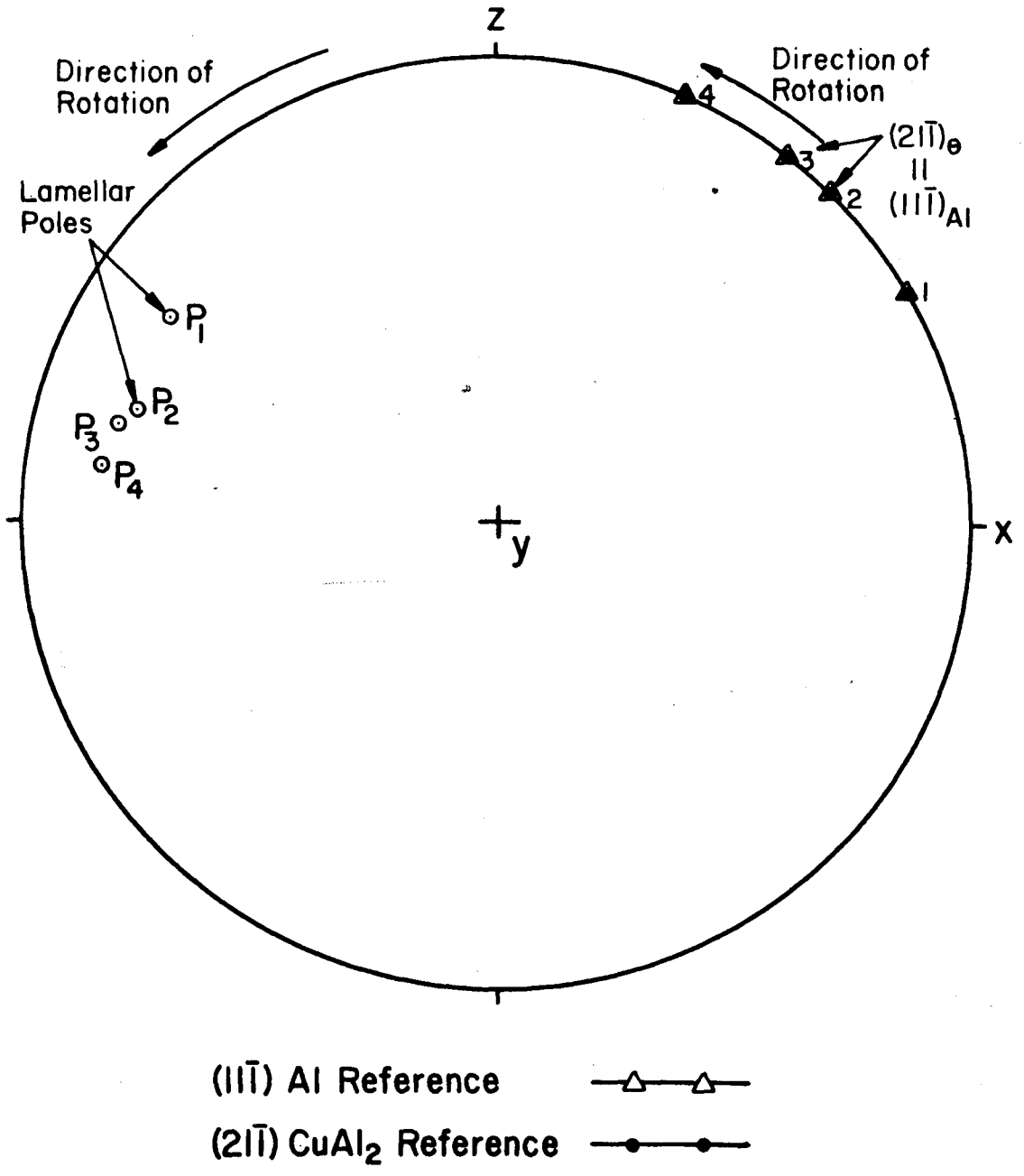

Fig. 11 Stereogram showing the orientation relationship and the lamellar interface normals in Ingot I. The structure twists around the ingot axis Y.

T

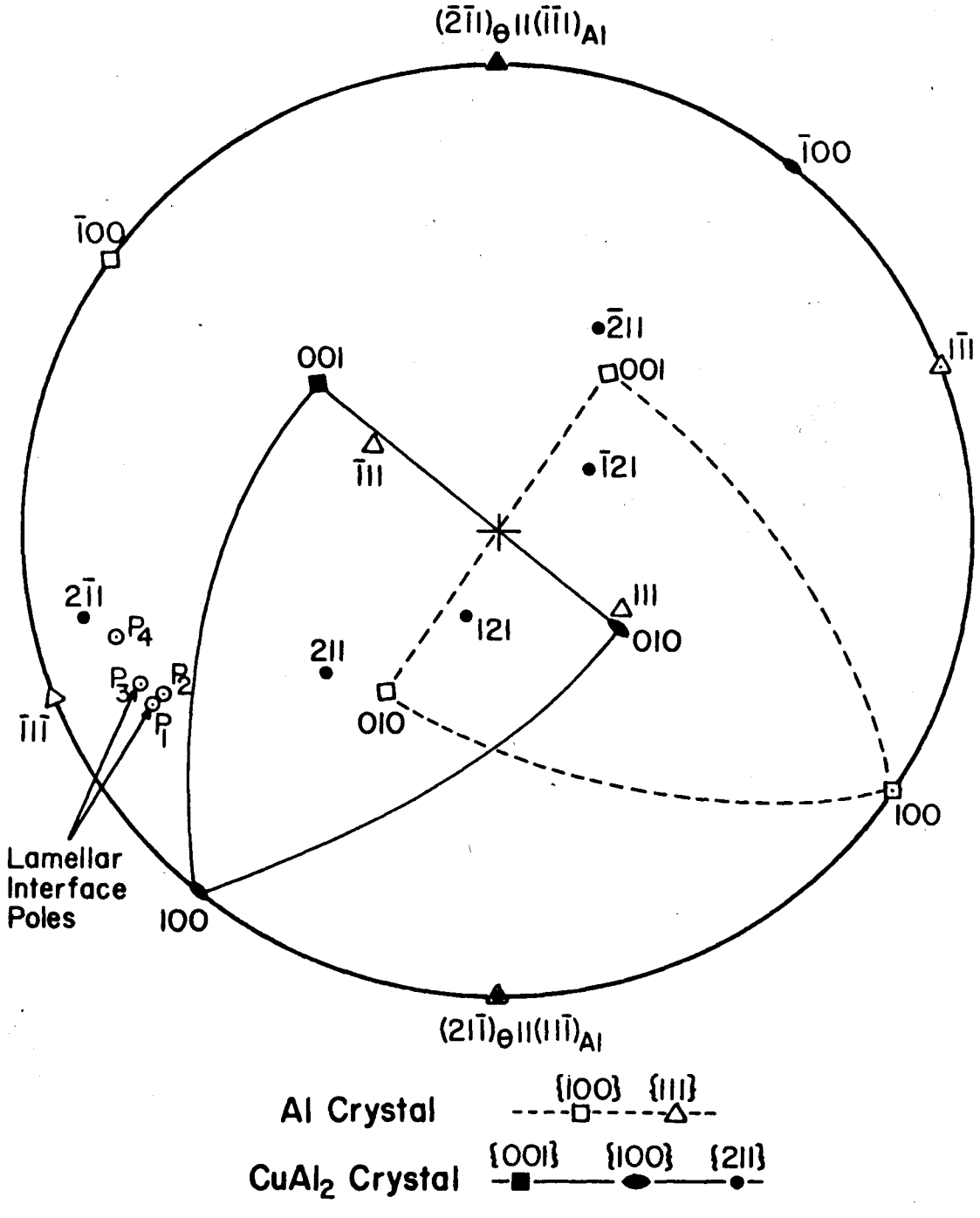

Fig. 12 Stereogram showing the position of lamellar interface normals in Ingot I.

	INGOT 1				INGOT 2			
	θ_1	θ_2	θ_3	θ_4	θ_1'	θ_2'	θ_3'	θ_4'
Angular position of the transverse sections in degrees	23	35	47	60	33	45	61	77
Distance from the head end of the ingot of the T.S. in cms.	2.8	4.26	5.73	7.3	4	5.6	7.5	9.4
Symbol for interface normals in stereograms	P_1	P_2	P_3	P_4	P_1'	P_2'	P_3'	P_4'
Angle between lamellae trace and Z axis $\emptyset$ in degrees	59	45	38	24	64	53.5	41.5	27
Angle between lamellae trace and X axis ψ in degrees	12.5	13	12	10	14	13.6	13.8	12

Table I. This table lists the positions of the transverse sections from the curved ingots used for the two surface and TEM analyses. The data from the two surface analysis are also listed.

REFERENCES

1. Rosenhain, W. and Tucker, P.A., Phil. Trans. Roy. Soc. 1909, Ser A., vol. 209, p. 89.

2. Hogan, L.M., Kraft, R.W., and Lemkey, F.D., "Eutectic Grains," Chapter 5 (1970) Advances in Materials Science, Ed. by H. Herman, John Wiley and Sons, Inc.

3. Flemings, M.C., "Plane front solidification of polyphase alloys" (1974), p. 93. Solidification Processing. McGraw-Hill, Inc.

4. Kerr, H. W., Winegard, W. C., J. Metals, 1966, vol. 18, p. 565.

5. Tiller, W. A., "Polyphase Solidification" (1958) p. 276, Liquids Metals and Solidification, ASM, Cleveland Ohio.

6. Lemkey, P. D., Hertzberg, R. W., and Ford, J. A.,Trans. Met. Soc. AIME. (1965), vol. 233, p. 334.

7. Salkind, M. J., Lemkey, F.D., and Gedruf, F. D., "Whisker Composites by Eutectic Solidification," Chap. 10, (1969), Whisker Technology, Ed. A. Levitt, John Wiley and Sons, N.Y.

8. Thompson, E. R., and Lemkey, F.D., Metallic-Matrix Composites," in Composite Materials, Vol. 4, Ed. by K. G. Kreider, 1974.

9. Bibring, H., Conference on In-Situ Composites, vol. 2, p. 1. Sept. '72. Lakeville, Connecticut.

10. Kraft, R. W., J. Metals, (1966), vol. 18, p. 192.

11. Galasso, F. S., Douglas, F. C., and Batt, J. A. J. Metals, (1970) vol. 6, p. 40.

12. Bever, M. B., Duwez, P. E., and Tiller, W. A., Mat. Sci. Eng. (1970) vol. 6, p. 149.

13. Graham, L. D., Conference on In-Situ Composites, vol. 1, p. 107, Sept. '72, Lakeville, Connecticut.

14. Jackson, K. A., and Hunt, J. D., Trans. Met. Soc. of AIME, (1966), vol. 236, p. 1129.

15. Hunt, J. D., Clinton, J. P., J. Inst. Metals, (1962-63), vol. 91, p. 338.

16. Frank, F. C., Puttick, K. E., Acta. Met., (1956), vol. 4, p. 206.

17. Cooksey, D. J. S., Munson, D., Wilkinson, M.P., Hellawell, A., Phil. Mag., (1964), vol. 10, p. 745.

18. Taylor, P. J., Kerr, H. W., Winegard, W. C., Can. Met. Quart. (1964), vol. 3, p. 235.

19. Jaffrey, D., Chadwick, G. A., J. Inst. Met., (1969), vol. 97, p. 118.

20. Yue, A. S., J. Inst. Met., (1963-64), vol. 92, p. 248.

21. Cooksey, D. J. S., Day, M. G., Hellawell, A., (1967) p. 151, "Crystal Growth," Pergamon Press.

22. Chadwick, G. A., J. Inst. Metals, (1962-63), vol. 91, p. 298.

23. Chadwick, G. A., Progr. Mats. Sci., 1963, vol. 12, p. 97.

24. Day, M. G., and Hellawell, A., J. Aust. Inst. of Metals, (1964), vol. 9, p. 213.

25. Hunt, J. D., J. Inst. Metals, (1966), vol. 94, p. 125.

26. Straumanis, M., Brakss, N., Z. Phys. Chem. (1937-38), B 38-39, p. 140.

27. Ellwood, E. C., and Bagley, K. O., J. Inst. Metals (1949), vol. 76, p. 63).

28. Thompson, E. R., and Lemkey, F., Trans. ASM, (1969), vol. 62, p. 140.

29. Chadwick, G. A., and Jaffrey, D., Trans. AIME, (1970), vol. 1, p. 3389.

30. Garmong, G., Rhodes, C. G., Spurling, R. A., Trans. AIME, (1973), vol. 4, p. 707.

31. Lemkey, F. D., Hertzberg, R. W., and Ford, J. A., Trans. AIME, (1965), vol. 233, p. 334.

32. Breinan, E. M., Thompson, E. R., and Tice, W. K., Met. Trans. (1972), vol. 3, p. 211

33. Garmong, G., Trans. AIME, (1975),vol. 6A, p. 1335.

34. Garmong, G., Trans. AIME, (1976), vol. 5, p. 1257.

35. Barrett, C., Marsalski, J. P., "Structure of Metals," p. 45. McGraw-Hill Book Co., N.Y.

36. Kraft, R. W., and Albright, D. L., Trans. Met. Soc. A.I.M.E., (1962), vol. 224, p. 1176.

37. Davies, I. G. and Hellawell, A., Phil. Mag. (1969), vol. 19, p. 1285.

38. Kraft, R. W., Trans. AIME, (1962), vol. 224, p. 65.

39. Truelove, P., Double, D. D., Hellawell, A., J. Crystal Growth, (1968), vol. 2, p. 191.

40. Hopkins, R. H., and Stewart, A. M., Phil. Mag. (1970), vol. 22, p. 199.

41. Double, D. D., and Hellawell, A., J. Crystal Growth, (1969), ser 8, vol. 19, p. 107.

42. Kraft, R. W., Trans. Met. Soc. AIME, (1962), vol. 224, p. 65.

43. Hopkins, R. H., and Kraft, R. W., Trans. Met Soc. AIME, (1968), vol. 242, p. 1627.

44. Fletcher, N. H., and Adamson, P. L., Phil. Mag. (1966), vol. 14, p. 99.

VITA

Ravinder C. Verma was born on March 24, 1951 in Bombay, India. He attended Don Bosco High School and graduated in June '67. In September 1969 he entered the College of Engineering, Poona and majored in Metallurgy and Material Science, graduating in June '73.

In September 1973, Mr. Verma began graduate study in Metallurgy and Material Science at Lehigh University as a Research Assistant under the supervision of Dr. R. Wayne Kraft. Mr. Verma is currently a student member of the American Society of Metals and the Metallurgical Society of AIME.